JOURNAL OF MATERIALS SCIENCE: MATERIALS IN MEDICINE 4 (1993) 300–304

Interfacial tissue response to bioactive glasses with reduced surface reactivity

E. SCHEPERS, M. DE CLERCQ
Department of Prosthetic Dentistry, Catholic University of Leuven, Capucijnenvoer 7, 3000 Leuven, Belgium

P. DUCHEYNE
Department of Bioengineering, University of Pennsylvania, Philadelphia, USA

Bone bonding of surface active glasses paralleled compositional changes of the reacting glass surface. These reaction layers, however, were susceptible to mechanical failure upon loading. The objective of the current work was to study the relationship between the kinetics of the thickness of the interfacial layers and the glass composition. Specifically the composition was changed by adding CaF_2 and by increasing the SiO_2 concentration. Three samples of each of five glass compositions were implanted in the partial edentulous jaws of beagle dogs. After 3 months, they were resected and prepared for histological analysis with the implants *in situ*. Bone bonding was observed at the surface of all five glass compositions. The glasses with low CaF_2 content showed large areas of bone bonding and the bone growth along the implant surface was enhanced by osteoconductivity. The bone bonding around glasses with high CaF_2 content was rather patchy. Small areas of bone bonding alternated with small islands of fibrous tissue contact. Osteoconductivity was observed also around these glass compositions. Scanning electron microscopy analysis revealed that the thickness of the reacted glass decreased with an increase of the CaF_2 concentration. The glasses with high CaF_2 concentrations showed spots of excessive ion dissolution which could delay the bone bonding in this area. This was due probably to local variations of the microstructure of the glass. CaF_2 addition increased the risk for crystallization of the glass. It was suggested that the interface boundaries between the crystalline and amorphous phases were more susceptible for ion dissolution.

1. Introduction

Bioactive glasses have been shown to bond to bone tissue [1–4]. This bone connection was associated with osteoconductivity, i.e. the propensity of bone tissue to grow along the material surface [3]. Eventually, this can result in a complete encapsulation of the bioactive glass surface by bone tissue, thus creating an excellent anchorage of the implant in the jaw bone.

The clinical use of bioactive glasses has so far been restricted to non-load bearing applications by virtue of the limited strength and fracture toughness of the glass. Whereas loaded hip prostheses with a bioactive glass coating have been partially successful at best [5], the use of bioactive glass implants in unstressed situations, such as the replacement of the ossicles within the middle ear have been implemented with success [6].

The mechanical properties of the bulk bioactive glass can be improved substantially by reinforcing the glass with ductile metal fibres [7]. Initially, stainless steel fibres were selected as the reinforcing material because of the close match between the thermal expansion coefficients of the bioactive glass and the metal fibres.

It appeared that this fibre-toughening of the glass rendered bioactive glass a structurally more reliable material. However, one still has to consider the strength of the reacted glass. The bonding of bioactive glass to bone tissue was associated with a series of chemical interactions at the interface with the surrounding fluids and tissues. Specifically, a silicon rich layer was formed on top of which a calcium phosphate rich layer was established. This phenomenon, which has been shown repeatedly and reproducibly both *in vitro* and *in vivo*, was the result of the open SiO_2 network structure of the glass. Upon surface dissolution of primarily the alkali ions, the Si-rich layer was probably a silica-gel, with low mechanical properties. It was recently shown that, even in the presence of an established glass–bone bond, this interfacial reaction zone was susceptible to shearing upon loading produced by the chewing forces.

Upon a topical shear failure of the reacted glass layer, the leaching reactions can continue and eventually might expose the underlying metal fibres. Experiments with this stainless steel fibre reinforced bioactive glass made it clear, though, that these fibres must remain covered by a rim of glass. A possible

0957–4530

exposure of the stainless steel fibres to the surrounding tissue fluids resulted in a release of ions or other compounds from the metals. These released moieties then interfered with the local osteogenesis possibly in a synergistic manner with the released glass ions [3, 4, 8].

In this study we addressed the issue of extensive surface reactivity by varying the composition of bioactive glass without hampering, however, its bone bonding capacity and osteoconductive properties. Specifically, the composition of the 'classic' 45–S–5 glass composition [1] was gradually altered by increasing the content of SiO_2, by decreasing the content of CaO and Na_2O and by adding CaF_2.

2. Materials and methods

Four new glass compositions were selected for implantation purposes together with the 45–S–5 bioactive glass which served as the reference material. Table I summarizes the nominal compositions.

The powder components were mixed, pressed into pellets, melted and homogenized in a covered platinum crucible at 1350 °C for 12 h. The glass was poured into graphite moulds and slowly cooled to room temperature at a rate of 0.7 °C min^{-1} to avoid residual stresses. The glass samples were then machine made into cylinders of 4 mm diameter and length 8 mm. The glass cylinders were sterilized in ethylene oxide and degassed for at least 48 h.

Three samples of each glass composition were implanted at random in the partial edentulous lower jaws of two beagle dogs under premedication with a neuralept-analgeticum (Hypnorm, Duphar, Amsterdam, The Netherlands), and anaesthesia with a pentobarbital (Nembutal, Ceva, Brussels, Belgium), according to the prescriptions of the manufacturers. The bone cavities were prepared with internally cooled low speed rotating instruments. The gingiva was sutured with non-resorbable silk, and antibiotics (Penadur LA) were administered immediately postoperative and at 3 days. The dogs were put on a soft diet during the healing period of the gingiva and returned to the normal standard food after removal of the sutures.

For comparability with previous experiments [3, 4, 8], the jaws were resected after three months of implantation and fixed immediately in a solution of neutralized formaldehyde and ethanol. The specimens were dehydrated in a series of graded ethanol solutions up to absolute ethanol, soaked in purified methylmethacrylate monomer and finally polymerized. Sections of approximately 100 μm were made on a sawing microtome (Leitz 1600. Wetzlar, Germany).

TABLE I Components of the glasses (by weight)

	SiO_2	CaO	CaF_2	Na_2O	P_2O_5
45–S–5	45	24.5	0	24.5	6
45–S–5–F–4	45	12.25	12.25	24.5	6
52–S–4.6–F	52	10.50	10.50	21	6
FX	52	16	16	10	6
FY	52	18.50	18.50	5	6

The sections were always made in the bucco-lingual direction parallel to the long axis of the implants. The final thickness of the sections (approximately 30 μm) was obtained by grinding and polishing with SiC paper up to 1200 grit using watercooling in a semi-automatic way (Minimet, Buehler, Lake Bluff, IL).

The sections for light microscopy were stained with Giemsa's staining solution and Paragon. The sections for scanning electron microscopy (SEM) and electron microprobe analysis (EMA) were covered by a thin, approximately 10 nm thick carbon layer. The thickness of the reacted glass layer was determined by scanning electron micrograph images obtained in the back-scattered electron imaging mode.

Bone bonding at the implant surface was quantified by morphometrical analysis on two sections of each implant and since three samples of each glass composition were implanted, six sections of each glass composition were evaluated. The ratio between the length of the bone bonding at the implant surface and the initial contact length between the cortical bone and the implant surface was calculated following a method extensively described previously [3].

3. Results

Bone bonding was observed at the surfaces of all five glass compositions. The osteocytes were distributed regularly along the glass surfaces and were in a close relationship with the reacted glass layers. Normal Haversian systems were present in the bone tissue at the interface.

The 45–S–5, 45–S–5–F–4 and 52–S–4.6–F glasses showed bone apposition along a large portion of their surfaces. These areas were preferentially located in the contact areas with the cortical bone. From these initial sites of bone bonding, the bone connection along the implant surface was extended by the osteoconductive properties of the glasses. Eventually this could result in a glass surface which was completely surrounded by bone tissue (Fig. 1). In the vicinity of the infra-alveolar nerve-vessel bundle the glass surface was surrounded by fibrous tissue. The collagen fibres were packed densely and in most places oriented parallel to the glass surface. Fibroblasts were rather scarce and in-

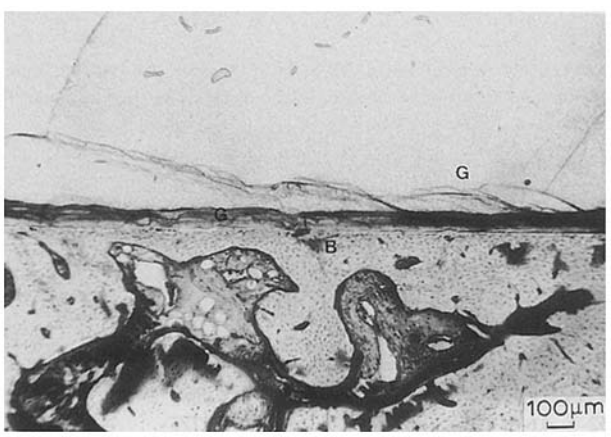

Figure 1 Micrograph of a 45–S–5 sample. The glass surface (G) was entirely covered by bone tissue (B).

flammatory cells were absent. In some areas, these fibres had an oblique orientation which might indicate a connection to the glass surface (Fig. 2). The 45–S–5, 45–S–5–F–4 and 52–S–4.6–F glasses showed a uniformly reacted glass layer (Table II).

The FX and FY glasses also showed bone bonding, but the bone bonding areas were rather small and patchy and they alternated with areas of fibrous tissue contact (Fig. 3). The bone bonding capacity of these glasses was demonstrated by osteoconductive bone growth and by the presence of large areas of osteoid tissue (Fig. 4). The surfaces of the reacted FX and FY glasses had a rather irregular appearance since they reacted more intensively in some areas than in others (Fig. 5). These differences in intensity of the interfacial reactions corresponded with the patchy bone bonding areas. In areas where the glass had reacted slightly and uniformly, bone bonding was present. In the vicinity of the intensively reacted parts of the glass surface fibrous tissue and some phagocytotic cells could be detected (Fig. 6). At the transition between intensively and slightly reacted glass areas, large bands of osteoid tissue and numerous osteoblasts were present.

Back-scattered imaging of the various glass composition revealed the existence of a dual reaction layer at the surface of each implant. This dual reaction layer consisted of a Si-rich layer covered by a CaP-rich layer (Fig. 7). The differences of the thickness of the reacted glass layers is summarized in Table III. The first group, the 45–S–5, 45–S–5–F–4 and 52–S–4.6–F glasses, showed a uniform and homogeneous reacted glass layer but the thickness of this reacted layer decreased gradually from 165 μm to 150 μm and 90 μm, respectively. In the second group, the FX and FY glasses, the glass layer was no longer homogeneous and uniform but it showed spots of excessive ion

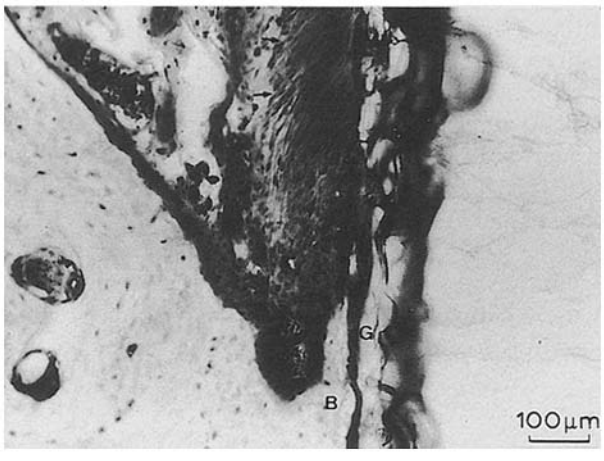

Figure 2 Micrograph of a 52–S–4.6–F sample. Above the bone bonding (B) to the glass surface (G) the fibres (↑) showed an oblique orientation to the glass surface.

TABLE II Morphometrical results: ratio between the length of bone bonding and the initial contact length between cortical bone and the implant surface

	Mean value	Standard deviation
5–S–5	1.160	0.1998
45–S–5–F–4	1.445	0.4682
52–S–4.6–F	1.240	0.2775
FX	0.607	0.3257
FY	0.782	0.1774

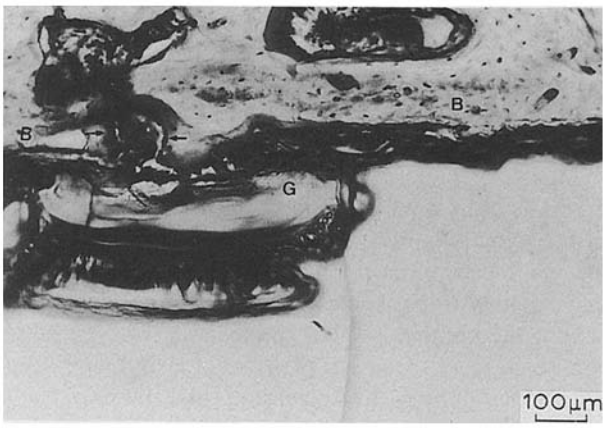

Figure 3 Micrograph of a FX sample. At the glass surface (G) areas of bone bonding (B) alternated with areas of fibrous tissue contact (↑).

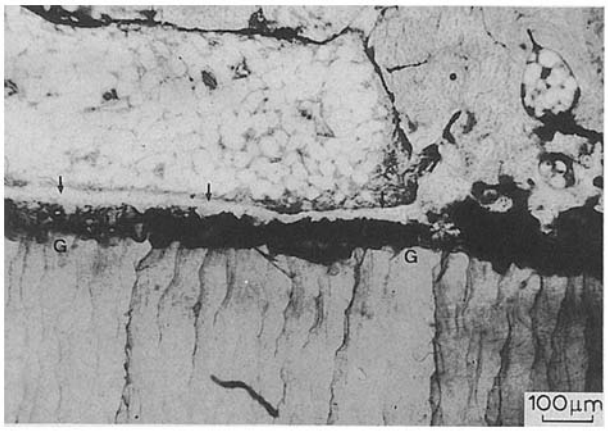

Figure 4 Micrograph of a FY sample. Osteoconductive bone growth (↑) along the glass surface (G) was demonstrated.

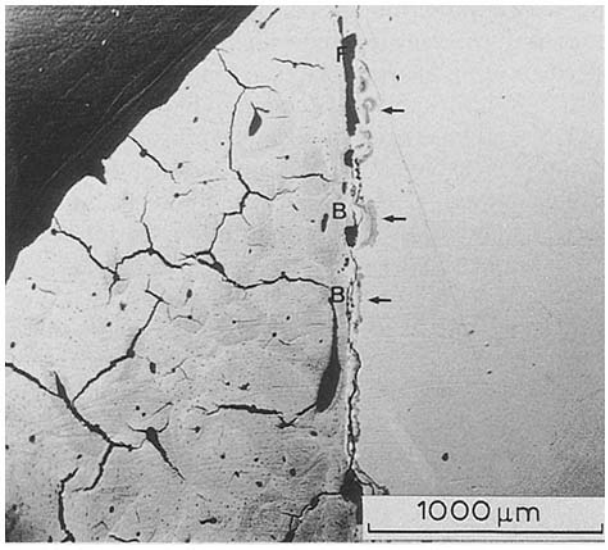

Figure 5 Back-scattered electron micrograph of a FX sample. The glass showed an irregular reacted surface (↑). Bone bonding area (B) alternated with fibrous tissue (F) spots at the interface.

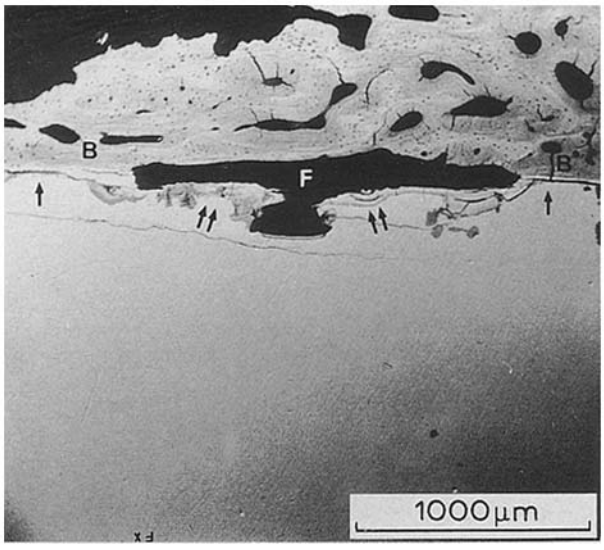

Figure 6 Back-scattered electron micrograph of a FX sample. In areas with a slightly reacted surface (↑) bone (B) bonded to the surface. In areas with an intensively reacted surface (↑↑) fibrous tissue (F) was observed at the interface.

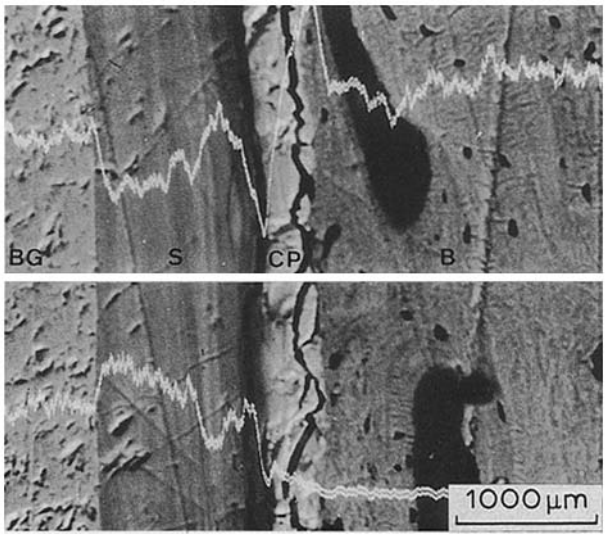

Figure 7 Back-scattered electron micrograph of a 45–S–5–F–4 sample with superimposed line-scans of the Ca content (CA) and Si content (SI). BG = bulk glass, S = Si-rich layer, CP = CAP-rich layer, B = bone tissue.

TABLE III Thickness of reacted glass layers

Glass type	Thickness (µm)
45–S–5	165
45–S–5–F–4	150
52–S–4.6–F	90
FX	30–370
FX	25–150

dissolution. In these areas the glass reacted up to a depth of approximately 370 µm for the FX glass and up to approximately 150 µm for the FY glass. However, in the deeper parts of those excessively dissolved areas osteoid tissue and active osteoblasts could be detected (Fig. 8).

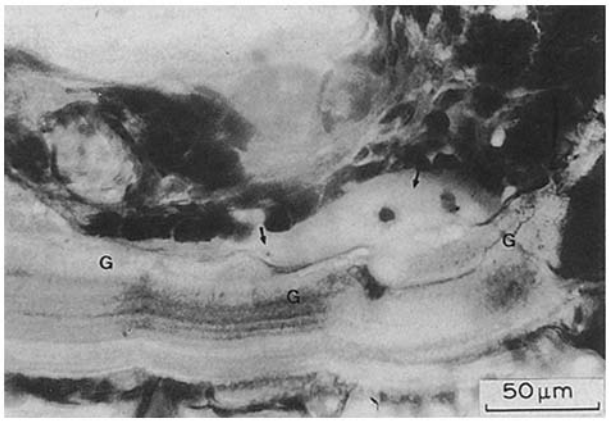

Figure 8 Micrograph of a FX sample. In the deeper parts of the excessively reacted area (G) osteoid tissue (↑) could be detected.

4. Discussion

In the present study the composition-dependent reduction of the reactivity of bioactive glasses was determined. Thus the CaO concentrations were decreased, as well as the Na_2O concentrations. At the same time CaF_2 was proportionally added. In three glass compositions the SiO_2 concentration was raised from 45 wt % to 52 wt %.

In the morphometrical results the glasses could be divided in two groups, the first one consisting of the 45–S–5, 45–S–5–F–4 and 52–S–4.6–F glasses and the second one consisting of the FX and the FY glasses. In the first group the mean value of bone bonding at the surface was larger than one. Here bone tissue had bonded almost entirely to the glass surface in the contact area with cortical bone. From these areas bone started to grow along the implant surface in the cervical and apical direction. In the spongeous bone the osteoconductive growth started from the initial contact spots with bone trabeculae. The second group had a mean value of bone bonding smaller than one and showed a patchy bone bonding behaviour, which corresponded with the irregular reacted glass layer. Nevertheless, stimulation of bone bonding by osteoconductivity could be detected.

The bone bonding ability of a given glass composition was determined by the ratio between the network former (SiO_2) and the network modifiers (CaO and Na_2O) [9]. By increasing the concentration of SiO_2 and, or decreasing the concentration of Na_2O, this ratio would increase, thereby stabilizing the three-dimensional network and retarding the ion dissolution and exchange.

The bone bonding ability of a bioactive glass was preserved when the SiO_2 concentration of the glass varied between 42 wt % and 55 wt %. The ratio of Na_2O to CaO could vary considerably without hampering the bone bonding capacity of the glass [9, 10], and furthermore the concentration of Na_2O could be substantially decreased without losing the bone bonding capacity [2]. The findings with the new glass compositions studied here confirmed the observations related to the SiO_2 and Na_2O content made in previous experiments [2, 9, 10].

The third variable in the present study was the partial substitution of SiO_2, CaO and Na_2O by CaF_2. In an *in vivo* study, Stanley *et al.* [11] reported bone bonding for fluoride containing bioactive glasses. Initial data were also presented which indicated that the inclusion of CaF_2 in a bioactive glass increased the rate of apatite film formation, affected the composition of this film, enhanced crystallization of the film and increased the film's resistance to demineralization [12]. *In vitro* measurements by Hench *et al.* [13] indicated that at a 40:60 ratio of CaF_2 to CaO, the formation of the apatite layer at the surface was optimized. In the current study it was shown that the same amount of CaF_2 and CaO, i.e. ratio equal to one, produced the greater osteoconductive effect, i.e. the 45–S–5–F–4 composition had a mean value of bone bonding at the surface which was considerably higher than for the 45–S–5 composition: 1.445 versus 1.16. A higher addition of CaF_2 at the expense of CaO and Na_2O, which was the case for the 52–S–4.6–F, FX and FY compositions, not only affected the chemical composition of the glass, but also its microstructure.

During the fabrication procedure of the different glass compositions the cast glass specimens were annealed at 650 °C for 4 h, and subsequently cooled to room temperature at a rate of 0.7 °C min^{-1}. Small white opaque spots could be observed in some of the fluoride-containing glass compositions, i.e. FX and FY. These spots were probably nuclei of a crystalline structure in the glass matrix.

The effect of nucleation treatments has been studied before *in vitro* and *in vivo*, specifically for non-CaF_2-containing bioactive glasses [1, 14]. It was observed, using X-ray diffraction, light and electron microscopy that there was no noticeable effect on the interfacial osteogenesis. Kokubo *et al.* [15] also used partially crystallized glasses (percentage of crystals up to 90%). For any of their compositions, a uniform reacted glass layer was observed both *in vitro* and *in vivo*. In contrast Gross *et al.* [16] showed a focal disintegration at the boundaries between the crystal phase and the glass matrix in several of the glass–ceramic compositions they studied.

In our experiment, the volume fraction and the size of the crystals were influenced by the duration of the thermal treatments. It was possible that the annealing treatment of the present study was conducive to crystallization and that the glasses were eventually partially crystallized. But more importantly, the presence of F^- ions affected nucleation of the crystalline phase very significantly. The implantation of the present partially crystallized glasses resulted in a severe attack at the interface boundaries between the crystalline and glass phase. This could explain the excessive ion dissolution in some areas of the FX glass surface, and its subsequent effect on the interfacial osteogenesis. However, osteoid tissue and active osteoblasts were still present in these areas, which indicated that the interfacial osteogenesis was not necessarily inhibited.

It thus appeared that the effect of crystallization on bioactive behaviour *in vivo* was not uniform and certainly could not be predicted on the basis of crystallization alone. In our experiments with a possible critical influence of fluorides, there was a uniform reactivity in compositions with at least 20% of Na_2O, but there was an inhomogenous reaction for compositions with 10% (or less) Na_2O.

5. Conclusions

1. All glass compositions showed bone bonding and osteoconductive properties.
2. The thickness of the reacted glass layers depended critically on the glass composition.
3. The presently analysed partially crystallized glasses were very susceptible to excessive ion dissolution producing a spotty form of interfactial osteogenesis.

References

1. L. L. HENCH, R. J. SPLINTER, W. C. ALLEN and T. K. GREENLEE, *J. Biomed. Mater. Res.* **2** (1971) 117.
2. U. M. GROSS and V. STRUNZ, *ibid.* **14** (1980) 507.
3. E. SCHEPERS, M. DE CLERCQ and P. DUCHEYNE, *J. Oral Rehabil.* **15** (1988) 473.
4. E. SCHEPERS, P. DUCHEYNE and M. DE CLERCQ, *J. Biomed. Mater. Res.* **23** (1989) 735.
5. P. DUCHEYNE, *ibid.* **19** (1985) 273.
6. R. RECK, *Clin. Otolaryngol.* **6** (1981) 63.
7. P. DUCHEYNE and L. L. HENCH, *Adv. Biomater.* **1** (1980) 21.
8. E. SCHEPERS, M. DE CLERCQ and P. DUCHEYNE, in "Implant materials in biofunction", edited by C. de Putter, G. L. de lange, K. de Groot and A. J. C. Lee (Elsevier Science Publishers, Amsterdam, 1988) p. 79.
9. M. WALKER and L. L. HENCH, U.S. Army Med. Res. Developm. Command DADA-17-70-C-001 #8,23-39 (1977).
10. A. E. CLARK, L. L. HENCH and H. A. PASCHALL, *J. Biomed. Mater. Res.* **10** (1976) 161.
11. H. R. STANLEY, L. L. HENCH, C. G. BENNETT, S. J. CHELLEMI, C. KING, R. GOING, N. J. INGERSOLL, E. C. ETHRIDGE, K. L. KREUTZIGER, L. LOEB and A. E. CLARK, *Int. J. Oral Implants* **2** (1982) 26.
12. D. B. SPILMAN, J. WILSON and L. L. HENCH, Transactions of the Second World Congress on Biomaterials, Washington, DC, (1984) p. 287.
13. L. L. HENCH, D. B. SPILMAN and D. R. NOLETTI, in "Biological and biomechanical performance of biomaterials", edited by P. Christel, A. Meunier and A. J. C. Lee (Elsevier Science Publishers B. V., Amsterdam, 1986) p. 99.
14. T. K. GREENLEE, C. A. BECKHAM, A. R. CREBO and J. C. MALMBORG, *J. Biomed. Mater. Res.* **6** (1972) 235.
15. T. KOKUBO, S. ITO, Z. T. HUANG, T. HAYASHI, S. SAKKA, T. KITSUGI and T. YAMAMURO, *ibid.* **24** (1990) 331.
16. U. M. GROSS, J. BRANDES, V. STRUNZ, J. BAD and J. SELA, *ibid.* **15** (1981) 291.

Received 28 November 1991
and accepted 11 January 1993